ACS APPLIED NANO MATERIALS

www.acsanm.org

Article

Zein/MnO_2 Nanosheet Composites Integrated with a Smartphone for Colorimetric Sensors for On-Site Detection of Adulterants in Milk

Tamires dos Santos Pereira, Danilo Martins dos Santos, Rafaela da Silveira Andre, and Daniel Souza Correa*

Cite This: *ACS Appl. Nano Mater.* 2024, 7, 13701−13711

Read Online

ACCESS | Metrics & More | Article Recommendations | Supporting Information

ABSTRACT: Milk and its derivatives are essential sources of nutrients for humans. However, the widespread adulteration of milk poses a significant challenge for ensuring the safety and integrity of these products. Here, a zein/manganese dioxide nanosheet (MnO_2 NS) composite-based colorimetric sensor integrated with a smartphone platform was developed for on-site and quantitative analysis of hydrogen peroxide (H_2O_2) and lactic acid, two common adulterants in milk samples. Sensing platforms were fabricated by spraying composite solutions onto various cost-effective and environmentally friendly substrates, including filter paper and masking tape, using a simple airbrush system. These platforms displayed remarkable sensitivity and suitable limit of detection (LOD) of 7.2×10^{-4} mol L^{-1} for H_2O_2 and 7.5×10^{-4} mol L^{-1} for lactic acid, respectively. These concentrations fall within the ranges established by diverse international regulatory bodies responsible for quality assurance protocols. Therefore, the dual detection of H_2O_2 and lactic acid in milk samples was successfully achieved in a rapid and cost-effective way, which opens possibilities for the design and implementation of field-deployable sensors for food safety surveillance and quality control.

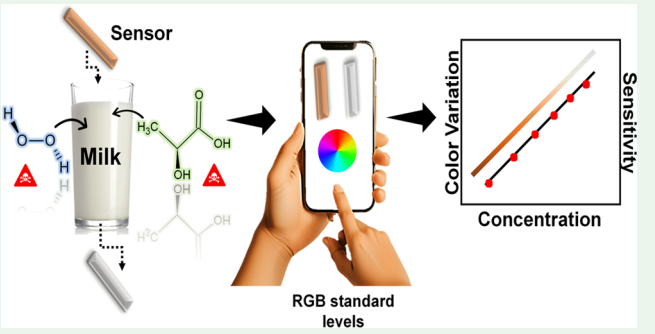

KEYWORDS: *food safety, quality control, hydrogen peroxide, lactic acid, functional nanomaterials*

1. INTRODUCTION

Milk and its derivatives are essential for human nutrition due to their high content of protein, carbohydrates, fats, and vitamins.[1] As a result, the consumption of these foods should be regularly incorporated into one's diet. The Food and Agriculture Organization (FAO) of the United Nations reported that global milk production reached 930 million tons in 2022.[2] Therefore, ensuring that milk meets the standards of quality and food safety is essential for fulfilling consumer needs. However, the practice of milk adulteration has unfortunately increased over the years as a strategy to reduce production costs and increase profits.[3] Milk adulteration can be categorized into three types: (i) adulteration of total nonfat solids, (ii) adulteration of fat content, and (iii) adulteration to extend the shelf life.[3] Common substances added to the first category include melanin and urea, whereas vegetables or detergents may be added to manipulate the fat content.[1] To extend the shelf life of milk, preservatives such as formalin, potassium dichromate, benzoic acid, salicylic acid, and hydrogen peroxide (H_2O_2) are often used.[1,3−6] H_2O_2 is used in milk to activate the enzyme lactoperoxidase, which has antimicrobial properties and extends the shelf life of milk.[7] In this regard, monitoring the presence of H_2O_2 in milk is relevant, as this substance can reduce the nutritional value of food by destroying vitamins A and E, resulting in potential risks to public health.[8] Investigations have shown that exposure to H_2O_2 in both short- and long-term can lead to cellular damage and is associated with several diseases, including diabetes, cancer, and cardiovascular and degenerative diseases.[9−14] Therefore, it is crucial to develop analytical methods that are both simple and affordable while also providing rapid detection of H_2O_2. Additionally, when one evaluates the quality of milk in relation to freshness, an important indicator is the presence of lactic acid.[15] The production of acidifying metabolites in milk is primarily caused by the activity of mesophilic bacteria, which grow well at ambient temperatures.[16] Prompt and effective cooling of milk after milking can significantly reduce the growth of mesophilic bacteria.[16] The lactic acid concentration is an important indicator of milk quality, as it is produced by the fermentation of lactose by lactic bacteria. High levels of lactate anions in milk indicate refrigeration problems after milking. The early detection of spoilage through the measurement of lactic acid can enable timely interventions at the industrial processing stage, related to improved refrigeration or enhanced cleaning

Received: April 18, 2024
Revised: May 23, 2024
Accepted: May 24, 2024
Published: June 4, 2024

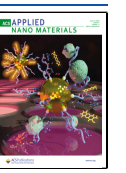

https://doi.org/10.1021/acsanm.4c02263
ACS Appl. Nano Mater. 2024, 7, 13701−13711

Scheme 1. Schematic of Colorimetric Sensor Development. (a) Zein-MnO_2 Solution; (b) Substrate Modification Using an Airbrush; (c) Detection of Adulterants in Milk; (d) Transduction of RGB Pattern Changes by a Smartphone. (e) Quantification of Analyte Concentration

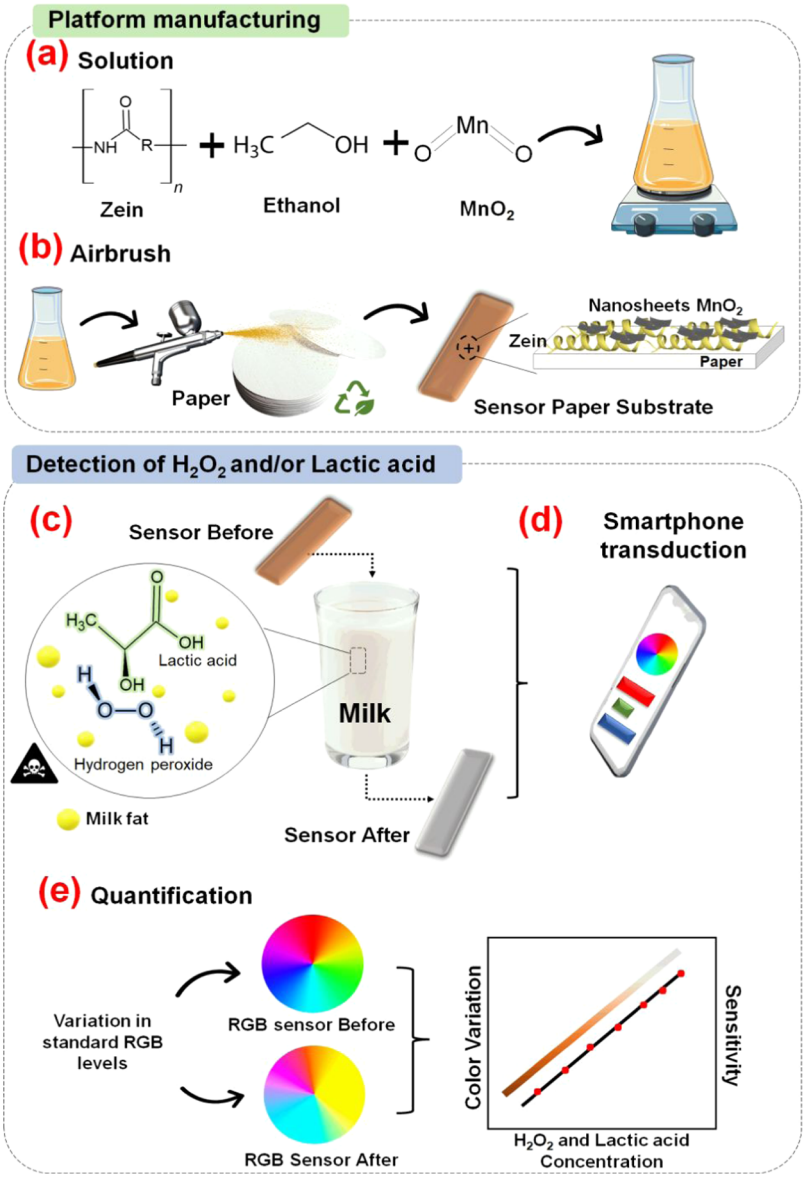

protocols. Therefore, lactic acid detection is extremely important to ensure consumer food safety.[17]

Colorimetric sensors are devices capable of detecting a target analyte by altering its maximum absorption wavelength, resulting in color change. The transduction mechanism of a colorimetric sensor depends on the change in light absorption of a chemochromic material.[18] Colorimetric sensors offer numerous advantages, including specificity, high sensitivity, cost effectiveness, ease of use, rapid analysis, straightforward operation, and clear visibility to the naked eye.[19,20] These sensors are typically composed of materials that undergo changes in their absorption band when exposed to the analyte of interest. In the past years, two-dimensional (2D) nanomaterials have attracted much attention due to their diverse properties, such as appropriate atomic-level thickness, high light absorption intensity, and large specific surface area, making them suitable for a wide range of applications, including colorimetric sensors.[21−26]

Manganese dioxide nanosheets (MnO_2 NSs) have attracted significant attention as a prospective platform for colorimetric sensing.[27−29] These nanostructures possess high surface area-to-volume ratio and an abundance of active sites, which can enhance their sensitivity and selectivity, particularly in the detection of hydrogen peroxide (H_2O_2).[30,31] Upon contact with H_2O_2, a redox reaction occurs, resulting in the formation of specific color changes.[32] This presents a straightforward and efficient method for detecting H_2O_2, which can be observed with the naked eye or analyzed using spectrophotometry.[32,33] Moreover, the facile synthesis and tunable properties of MnO_2 nanosheets make them versatile candidates for developing cost-effective and efficient colorimetric sensors for various applications, including environmental monitoring, biomedical diagnostics, and industrial processes.

Zein, a natural protein derived from corn, has emerged as a promising platform for colorimetric sensors as it offers the benefits of low cost, simplicity, and scalability.[34−36] By

https://doi.org/10.1021/acsanm.4c02263
ACS Appl. Nano Mater. 2024, 7, 13701−13711

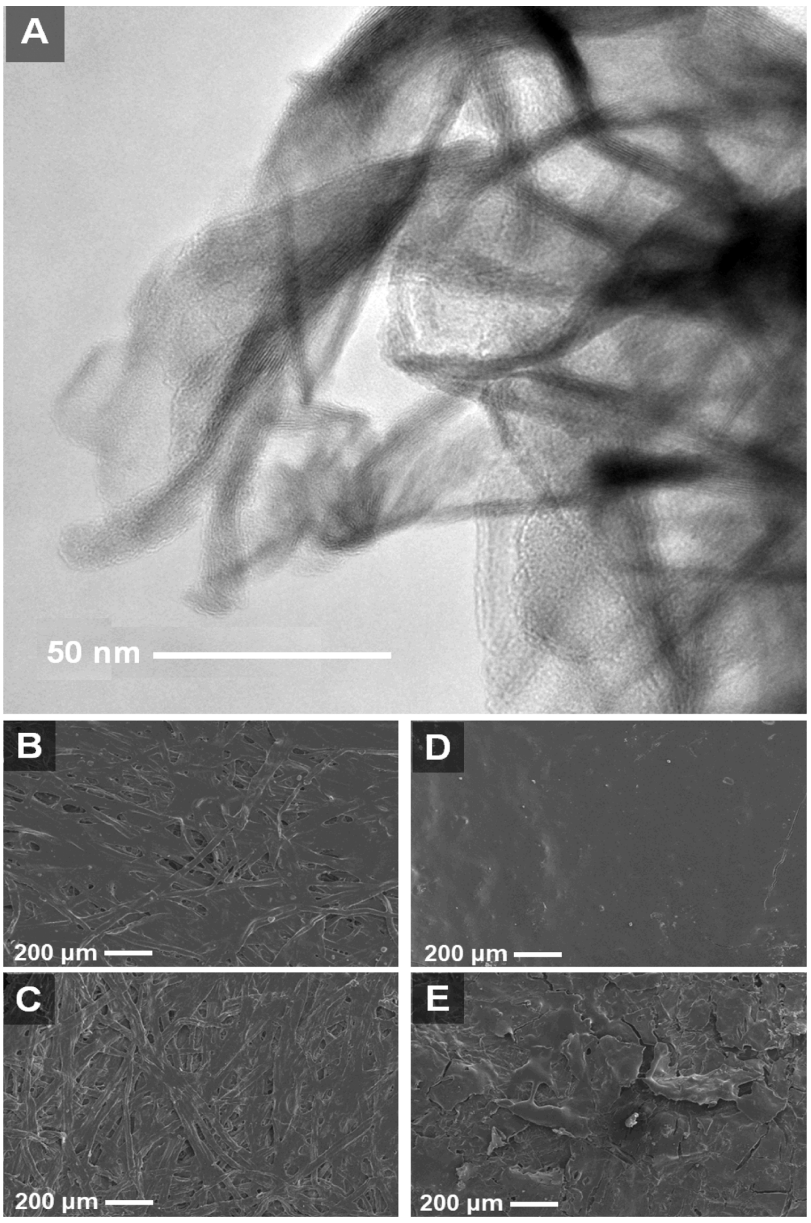

Figure 1. (A) TEM image of MnO_2 NSs. SEM images of the sensing platform on the paper substrate (B) before and (C) after H_2O_2 detection. SEM images of the sensing platform on the tape substrate (D) before and (E) after H_2O_2 detection.

immobilizing indicator components onto zein matrices, such as nanoparticles or dyes, sensitive and selective colorimetric sensors can be developed for detecting a wide range of analytes, including heavy metals, pathogens, and environmental pollutants.[35,36] The hydrogen bonds present in zein facilitate the formation of films through self-assembly,[33] enabling facile surface modification of diverse substrates. Additionally, the insolubility of zein in water makes it particularly suitable as a matrix material for colorimetric sensors, allowing its use in aqueous media without degradation concerns.[33]

Herein, MnO_2 NSs/zein composite was successfully employed to modify the surfaces of low-cost, recyclable, and easily accessible substrates, including paper, adhesive tape, and poly(ethylene terephthalate) (PET). The resulting platforms were utilized as colorimetric sensors for the identification of two milk contaminants, namely H_2O_2 and lactic acid, as illustrated in Scheme 1. To assess the sensing capabilities, colorimetric measurements were performed to analyze the variations in RGB color patterns. The results demonstrated the high efficiency of the platforms in detecting the target analytes. Essential morphological and structural characterizations were carried out to validate the composition of the composite material and to elucidate the reaction mechanisms involved in the detection process. These characterizations played a crucial role in confirming the successful incorporation of MnO_2 nanosheets and zein onto the substrates and understanding the underlying chemical processes driving the sensing mechanism.

2. MATERIALS AND METHODS

2.1. Synthesis of Manganese Dioxide Nanosheets (MnO_2 NSs). MnO_2 NSs were synthesized according to the procedure described in the literature.[37] Specifically, 150 mL of a 2×10^{-2} mol L^{-1} potassium permanganate aqueous solution (Sigma-Aldrich) was mixed with 40 mL of ethyl acetate (Sigma-Aldrich) and heated under reflux at 85 °C for 16 h. After this period, MnO_2 NSs were separated from the reaction medium using a decantation funnel and washed with

https://doi.org/10.1021/acsanm.4c02263
ACS Appl. Nano Mater. 2024, 7, 13701−13711

distilled water and absolute ethanol. Finally, the nanosheets were dried at 50 °C for 2 h and then stored in a desiccator.

2.2. Manufacturing of Colorimetric Sensing Platforms. To develop colorimetric sensors, readily available, low-cost, and recyclable substrates were selected, including quantitative filter paper (UNIFIL), cotton (Topz), PET (derived from used bottles), cardboard (derived from boxes), adhesive tape (3M), and gauze (3M). To modify the substrates, 1.5 g of zein was added to 4 mL of ethanol and the solution was stirred for 1 h. Next, 20 mg of MnO_2 was solubilized in 1 mL of dimethyl sulfoxide (DMSO; Sigma-Aldrich) and added to the zein solution, and the mixture was stirred for an additional 30 min (Scheme 1a). The zein and MnO_2 NS solution was then loaded into an airbrush system and sprayed directly onto one face of the substrate, which had been fixed vertically (Scheme 1b). In the subsidiary experiments, the working distance and the number of layers applied were optimized to achieve ideal results. Our experiments determined that a working distance of 10 cm (evaluated by visual inspection of the homogeneity of the deposited film) and applying four layers yielded the best results. The process was optimized based on the sensitivity response of the sensor at the lowest H_2O_2 concentration of the standard curve, as shown in Figure S1. The detection tests were conducted using concentrations corresponding to the standard curve of the target analytes. The sensor was then immersed in the solution for 15 min, as shown in Scheme 1c. The sensitivity was calculated using eq 1, which quantifies the variation in the RGB color patterns of the colorimetric sensor in response to the concentration of the analyte being investigated (1e).[38]

$$S_{RGB}\,(\%) = \frac{(R_a - R_b) + (G_a - G_b) + (B_a - B_b)}{R_a + G_a + B_a} \times 100 \quad (1)$$

where R_a, G_a, and B_a are the initial values of red, green, and blue, respectively, and R_b, G_b, and B_b are the values after H_2O_2 detection.

The RGB patterns were measured using a smartphone (Samsung Galaxy A7, 24MP camera) and an RGB Color Detector application ("RGB Color Detector, Apps on Google Play").[39] Additionally, a camera chamber was designed to control the lighting during image acquisition (Scheme 1d), which was obtained using a Fused Deposition Modeling 3D printer (Ender 3 V2, manufactured by Creality (Shenzhen, China)) and a PLA filament (3DLAB, Betim, Brazil). The camera chamber was manufactured through 3D printing to achieve a precise and secure fit onto the smartphone. At the opposite end, an opening was left for the introduction of sensory platforms after analyte detection.

2.3. Detection Test (Analytical Curve and Milk Sample). To conduct colorimetric detection of H_2O_2 and lactic acid, three sets of sensor platforms were employed. Analytical curves were constructed within specific concentration ranges: 1×10^{-5} to 1 mol L^{-1} for H_2O_2 and lactic acid. Analytical concentrations were selected in accordance with the regulatory thresholds established by oversight bodies such as the ANVISA (Brazil) and the FDA.[40−42] To ensure optimal performance, the platforms were immersed in the test solutions for 15 min. Next, they were removed from the solutions and left to air-dry at room temperature for 24 h. Following the completion of the drying process, RGB patterns were acquired by capturing images using a Samsung Galaxy A7 smartphone connected to a camera featuring controlled brightness settings. Subsequently, the obtained images were processed and analyzed using the RGB Color Detector application with the aid of eq 1.

To enhance the detection in milk samples, a saline phosphate buffer solution with a pH of 7.4 was prepared, totaling a volume of 100 mL at a concentration of 1×10^{-1} mol L^{-1}. For increased stability, 0.01 mL of Tween 20 stabilizer was carefully introduced into the solution. Subsequently, three types of samples were created using whole, semiskimmed, and skimmed milk, with 2 g of each type of milk added and the resulting mixture homogenized. For analytical purposes, solutions were spiked with various analyte concentrations. After dilution, the final concentrations were set to 1×10^{-5}, 1×10^{-4}, 1×10^{-3}, 1×10^{-2}, 5×10^{-2}, and 1 mol L^{-1} H_2O_2, lactic acid, or a combination of both analytes. The methodology employed to assess the variation in RGB patterns and conduct image acquisition was consistent with the previously described approach.

2.4. Morphological and Structural Characterization. Scanning electron microscopy (SEM) images were obtained using a JEOL JSM-6510 microscope at a voltage acceleration of 10 kV and different magnifications. Samples were fixed in sample holders using carbon tape and coated with gold using a sputter coater (Leica-SCD 050). Transmission electron microscopy (TEM) images of the MnO_2 NSs were obtained using a FEI Tecnai G2F20 microscope operated at an accelerating voltage of 200 kV. Fourier transform infrared (FTIR) spectra were obtained in ATR mode from 400 to 4000 cm^{-1} using a Bruker Vertex 70 spectrometer. Each spectrum was collected using 64 scans at a resolution of 2 cm^{-1}. FTIR analysis of the sensory platforms was performed before and after the detection of the product analytes. Thermogravimetric analysis (TGA) was performed using a thermogravimetric analyzer (Q500 TA Instruments) under a nitrogen atmosphere at a flow rate of 60 mL/min. Samples from the sensory platform and from each separate component were placed in platinum pans and scanned from 25 to 1000 °C at a heating rate of 10 °C/min.

3. RESULTS AND DISCUSSION

3.1. Morphological and Thermal Characterizations. MnO_2 nanosheets were successfully synthesized through the reaction between $KMnO_4$ and ethyl acetate, as shown in the TEM image (Figure 1A). The MnO_2 structures that were formed display nanoscale dimensions in terms of thickness (∼10 nm) and micrometer-scale dimensions in terms of length (2−5 μm).[37,43] Figure 1B,D displays the scanning electron microscopy (SEM) images of the sensors fabricated on paper substrate and adhesive tape substrate, respectively. In the case of the sensor on the paper substrate, the images revealed the presence of material fibers and an irregular surface. Conversely, the adhesive tape substrate exhibits a smoother and more uniform surface. In both cases, it was evident that the substrates were coated with zein layers, accompanied by clusters of MnO_2 NSs in certain regions. After subjecting the sensors to H_2O_2 detection, the morphological changes were evaluated, as shown in Figure 1C,E for the paper platform and adhesive tape, respectively. Upon exposure to the analytes, both sensors exhibited indications on their surfaces, suggesting consumption/degradation of both the nanosheets and zein films. Consequently, the fibers become more prominent on the paper substrate (Figure 1C), whereas the adhesive tape substrate (Figure 1E) displays an irregular surface and detachment of the applied coating used for modification.

Energy-dispersive X-ray spectroscopy (EDS) analyses were conducted on the MnO_2 sheets (Figure S2A), the paper substrate sensor (Figure S2B), and the sensor after the detection of H_2O_2 and lactic acid (Figure S2C,D, respectively). Mn and O were the predominant elements in the MnO_2 sheets. Regarding the sensor on the paper substrate, the presence of C from paper and zein, as well as N resulting from zein, and Mn and O due to the presence of MnO_2 sheets was noted. Upon exposure to the analytes, a decrease in the C, N, and Mn contents was observed. A comparison between the two analytes revealed a greater reduction in the Mn content after H_2O_2 detection, whereas a greater reduction in the N content was observed after lactic acid detection. This suggests distinct processes for detection mechanisms in the presence of each analyte. The zein/MnO_2 platform-based colorimetric sensor detects the presence of H_2O_2 and/or lactic acid by utilizing the catalytic activity of MnO_2 and the responsive behavior of zein. Upon exposure to H_2O_2 and/or lactic acid, a chemical reaction occurs between the target molecules and MnO_2, resulting in the reduction of the latter, which in turn causes a change in color, typically from brown to

https://doi.org/10.1021/acsanm.4c02263
ACS Appl. Nano Mater. 2024, 7, 13701−13711

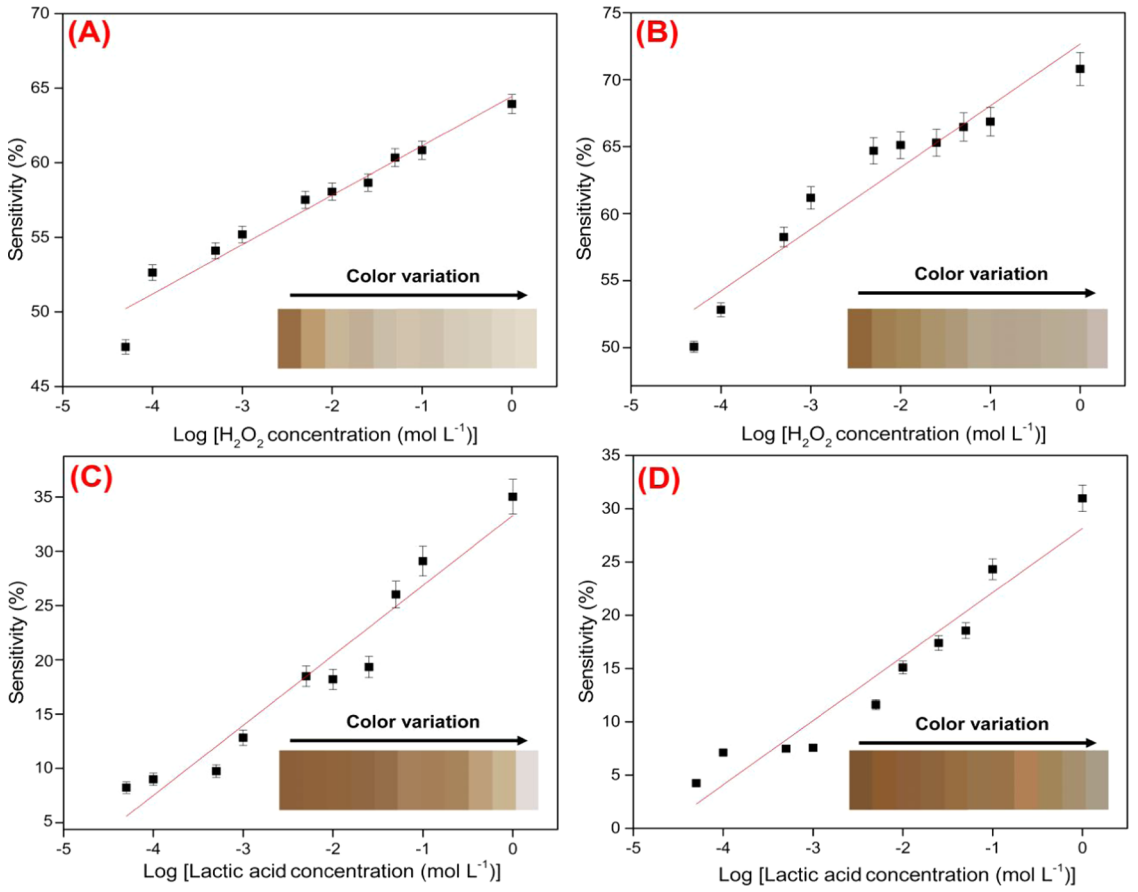

Figure 2. Sensitivity variation for (A) sensor on the adhesive tape substrate for the detection of H_2O_2. The linear equation sensitivity (%) = 3.30 (±0.27) × Log[H_2O_2] + 64.43 (±0.72), with a correlation coefficient of 0.9465 and LOD = 7.2×10^{-4} mol L^{-1}. (B) Sensor on the paper substrate for the detection of H_2O_2. The linear equation sensitivity (%) = 6.45 (±0.66) × Log [H_2O_2] + 45.72 (±1.74), with a correlation coefficient of 0.9221 and LOD = 8.9×10^{-4} mol L^{-1}. (C) Sensor on the adhesive tape substrate for the detection of lactic acid. The linear equation sensitivity (%) = 10.31 (±0.90) × Log [lactic acid] + 61.28 (±2.36), with a correlation coefficient of 0.9423 and LOD = 7.5×10^{-4} mol L^{-1}. (D) Sensor on the paper substrate for lactic acid detection. The inset in the images shows the color variation of the sensor. The linear equation sensitivity (%) = 6.01 (±0.58) × Log [lactic acid] + 8.14 (±1.52), with a correlation coefficient of 0.9305 and LOD = 8.3×10^{-4} mol L^{-1}.

colorless or from dark brown to light brown. This alteration in color can be visually observed or quantitatively measured using spectroscopic techniques. Moreover, zein serves as a stable matrix for immobilizing MnO_2 nanoparticles, enhancing the stability and sensitivity of the sensor. As zein dissolves faster in acidic medium, the presence of lactic acid triggers the dissolution of the zein matrix, facilitating the interaction between MnO_2 and the target molecules, thereby amplifying the colorimetric response.

TGA (Figure S3) was employed to examine the material composition in relation to the proportion of each constituent. Pure zein exhibited two weight losses, where the first occurred below 100 °C and was attributed to the removal of physically adsorbed water.[44,45] The second loss is associated with the decomposition of the main protein structure of zein, resulting from the breakage of low-energy intermolecular bonds.[44,45] The overall residue accounted for 14% of the total. The MnO_2 NSs displayed two distinct stages of mass loss. The first stage, ranging from 100 to 450 °C, was attributed to the elimination of adsorbed and crystalline water from MnO_2.[46,47] The second stage occurred beyond 500 °C, corresponding to structural alterations during the phase transition, wherein MnO_2 was transformed into Mn_2O_3 and subsequently to Mn_3O_4.[46,47] The final nanosheet residue was 82%. Two weight losses were observed in the paper substrate. The initial weight loss, below 100 °C, was ascribed to desorption of physically adsorbed water on the paper surface.[48,49] The second weight loss, occurring between 250 and 400 °C, was linked to the degradation of organic molecules containing hydrogen and carbon, leading to the disintegration of the cellulose framework.[48,49] No residue was detected for this substrate. Upon evaluating the paper/zein-MnO_2 sensor, two weight losses were observed. The first weight loss prior to 100 °C can be attributed to moisture evaporation. The second weight loss, ranging from 200 to 350 °C, is related to the previously reported degradation processes of zein and MnO_2 NSs. The resulting residue in the sensor was 8%. Considering the residues of each constituent individually, it can be inferred that for every 1.00 g of zein-MnO_2 solution deposited on the substrate, 0.14 g corresponded to zein and 0.82 g corresponded to MnO_2, with any remaining mass accounting for impurities.

3.2. H_2O_2 or Lactic Acid Detection. Figures 2 and S4 show the sensitivity and color variation of the sensors after exposure to various concentrations of H_2O_2. The analytical curve presents the sensitivity as a function of the log of the analyte concentration, and the adjustments for R^2 and the limit of detection (LOD) were calculated based on the linear section of the curve. The LOD was calculated using the equation LOD = $3.3 \times \sigma/S$, where S is the slope of the calibration curve and σ is the standard deviation of the response. The sensors manufactured on the adhesive tape substrate (Figure 2A) presented the

https://doi.org/10.1021/acsanm.4c02263
ACS Appl. Nano Mater. 2024, 7, 13701−13711

Table 1. Comparison of the Analytical Performance of Different Sensors for H_2O_2 and Lactic Acid Detection

transduction	subtract	modification	analyte	LOD (mol L^{-1})	ref.
digital image (RGB)	paper	peroxidase enzyme	H_2O_2	3.5×10^{-4}	Lima et al.[42]
digital image (RGB)	paper	Ag NP-alginate	H_2O_2	1×10^{-4}	Sharma et al.[52]
digital image (RGB)	paper	MnO_2 NSs	H_2O_2	7.2×10^{-4}	this work
UV/vis spectroscopy	copper nanosheets	nitrophenol	lactic acid	3.3×10^{-4}	Rattu et al.[50]
UV/vis spectroscopy	Au−Ag bimetallic	carbon dots	lactic acid	3.3×10^{-8}	Zhang et al.[51]
digital image (RGB)	paper	MnO_2 NSs	lactic acid	7.5×10^{-4}	this work

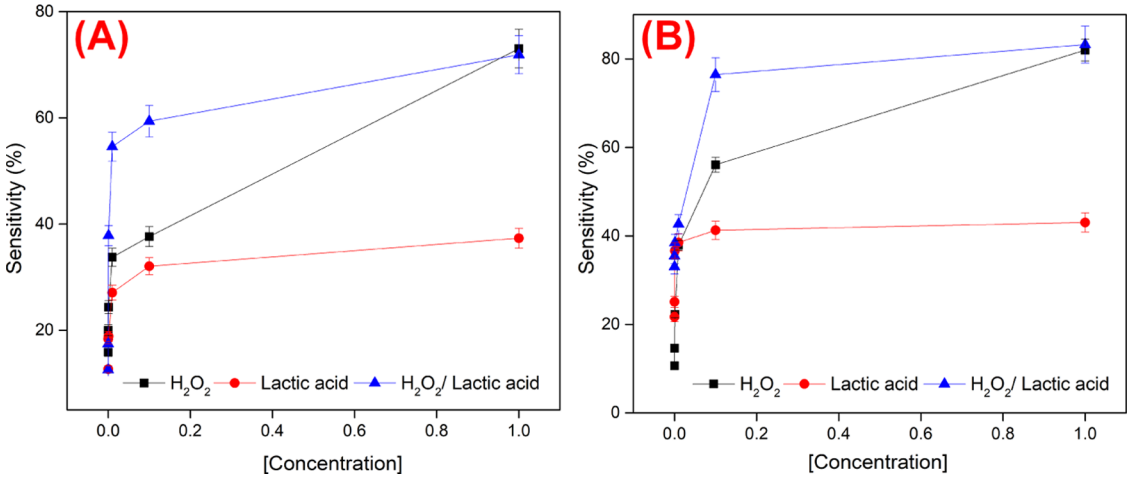

Figure 3. Dual variation in sensitivity as a function of the concentration of H_2O_2, lactic acid, and H_2O_2/lactic acid. (A) Sensor on a paper substrate and (B) sensor on an adhesive tape substrate.

linear equation sensitivity (%) = 3.30 (±0.27) × Log[H_2O_2] + 64.43 (±0.72), with a correlation coefficient of 0.9465 and LOD = 7.2×10^{-4} mol L^{-1} for H_2O_2 detection. In Figure 2B, the sensor on the paper substrate presented the linear equation sensitivity (%) = 6.45 (±0.66) × Log [H_2O_2] + 45.72 (±1.74), with a correlation coefficient of 0.9221 and LOD = 8.9×10^{-4} mol L^{-1} for H_2O_2 detection. Sensors with adhesive tape and paper substrates have been found to be better suited for routine analysis, offering greater durability and flexibility. Consequently, these two substrates were used for subsequent testing. It is important to note that the maximum allowable level of H_2O_2 in milk according to the US legislation aligned with the Food and Drug Administration (FDA) is 0.05% m/m.[40] Notably, the LOD achieved in this study for the determination of H_2O_2 is 0.001% m/m, which is below the currently established legal limit. In Brazil, ANVISA (National Health Surveillance Agency) regulations allow a maximum value of 0.3 g L^{-1} for H_2O_2 in milk samples, and therefore, our LOD of 0.024 g L^{-1} effectively satisfies this requirement.[41] Figure 2C,D shows the sensitivity and color change of the sensors exposed to different concentrations of lactic acid. The analytical curve presents the sensitivity as a function of the log of analyte concentration. For the detection of lactic acid, the sensor on an adhesive tape substrate (Figure 2C) presented the linear equation sensitivity (%) = 10.31 (±0.90) × Log [lactic acid] + 61.28 (±2.36), with a correlation coefficient of 0.9423 and LOD = 7.5×10^{-4} mol L^{-1}. In Figure 2D, the paper substrate-based sensor for acid detection presented the linear equation sensitivity (%) = 6.01 (±0.58) × Log [lactic acid] + 8.14 (±1.52), with a correlation coefficient of 0.9305 and LOD = 8.3×10^{-4} mol L^{-1}. The Brazilian regulatory agency ANVISA allows a maximum lactic acid concentration of 1.5×10^{-2} mol L^{-1}.[41] Therefore, the detection capacity of the proposed sensor was 18 times lower than the limit allowed by the Brazilian legislation.

The reproducibility of the sensor on a paper substrate was assessed under previously optimized conditions. Six distinct sensors were employed to detect concentrations of 1×10^{-1} mol L^{-1} of either lactic acid or H_2O_2. The relative standard deviations obtained for H_2O_2 and lactic acid detection were 5.07 and 5.09%, respectively. These values suggest that the detections can be reliably reproduced with acceptable variations. Repeatability tests were not feasible because of the single-use nature of each sensor.

When comparing our results with the available scientific literature, only two examples were identified in which colorimetric sensors were developed on paper substrates, employing smartphones as transducers to detect color variations for the H_2O_2 measurement (Table 1). Furthermore, there is a limited body of work on colorimetric sensors for lactic acid detection (Table 1). In terms of H_2O_2 detection, the LOD in our study is similar with other values reported in the literature. For lactic acid detection, our LOD matches that of Rattu[50] but remains higher than that of Zhang.[51] However, factors other than the LOD must be considered. For instance, here, a simple and portable transduction method that combines image capture via a smartphone was employed. Furthermore, flexible and environmentally friendly substrates that can be easily and quickly modified using only two low-cost components, namely zein and MnO_2 NSs, were utilized. These approaches result in a substantial reduction in operational and production expenses, while streamlining the analysis process.

3.3. H_2O_2 and Lactic Acid Dual Detection. To assess the selectivity of the sensor for each analyte, dual-detection experiments were conducted. Figure 3 shows three curves representing the sensitivity of the sensor in response to changes

https://doi.org/10.1021/acsanm.4c02263
ACS Appl. Nano Mater. 2024, 7, 13701−13711

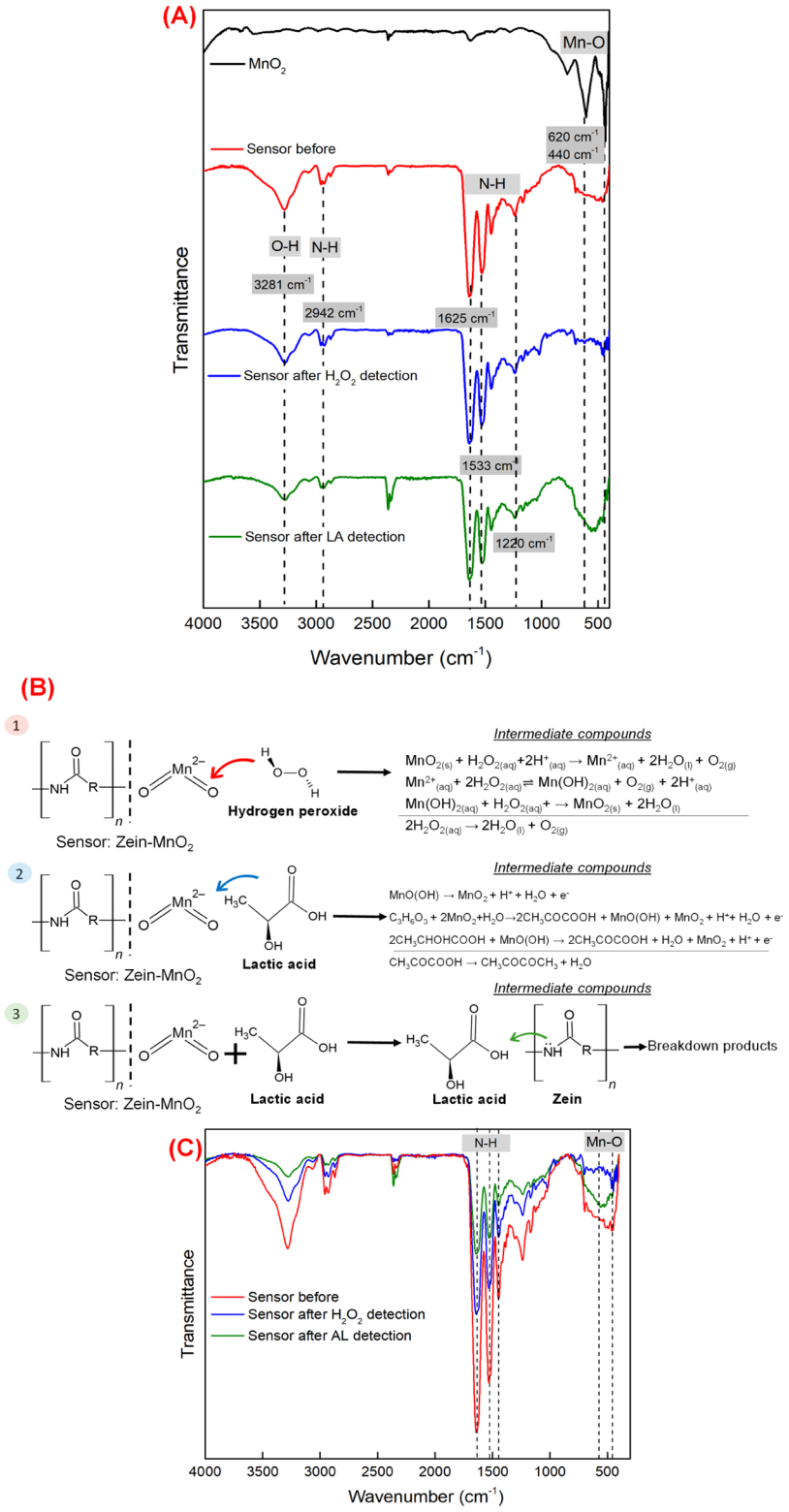

Figure 4. (A) FTIR spectra of the MnO_2 NSs (black curve), sensor on the paper substrate (red curve), and sensor after detection of H_2O_2 (blue curve) and lactic acid (green curve). (B) Reaction mechanism for H_2O_2 and lactic acid detection. (C) FTIR on the same magnitude scale for the sensor on the paper substrate (red curve) and sensors after the detection of H_2O_2 (blue curve) and lactic acid (green curve). The bands highlighted in the image correspond to the range from 1625 to 1220 cm^{-1} and the range from 440 to 621 cm^{-1}.

in RGB patterns during the detection of H_2O_2, lactic acid, or both at equivalent concentrations (Figure 3A,B). Our observations revealed that the sensor in contact with both analytes exhibited a higher sensitivity, especially at lower concentrations (Figure 3A,B). As the concentration increased, the sensor exposed solely to H_2O_2 also reached comparable sensitivity levels, whereas the sensor exposed solely to lactic acid displayed lower sensitivity than the others, regardless of the

https://doi.org/10.1021/acsanm.4c02263
ACS Appl. Nano Mater. 2024, 7, 13701−13711

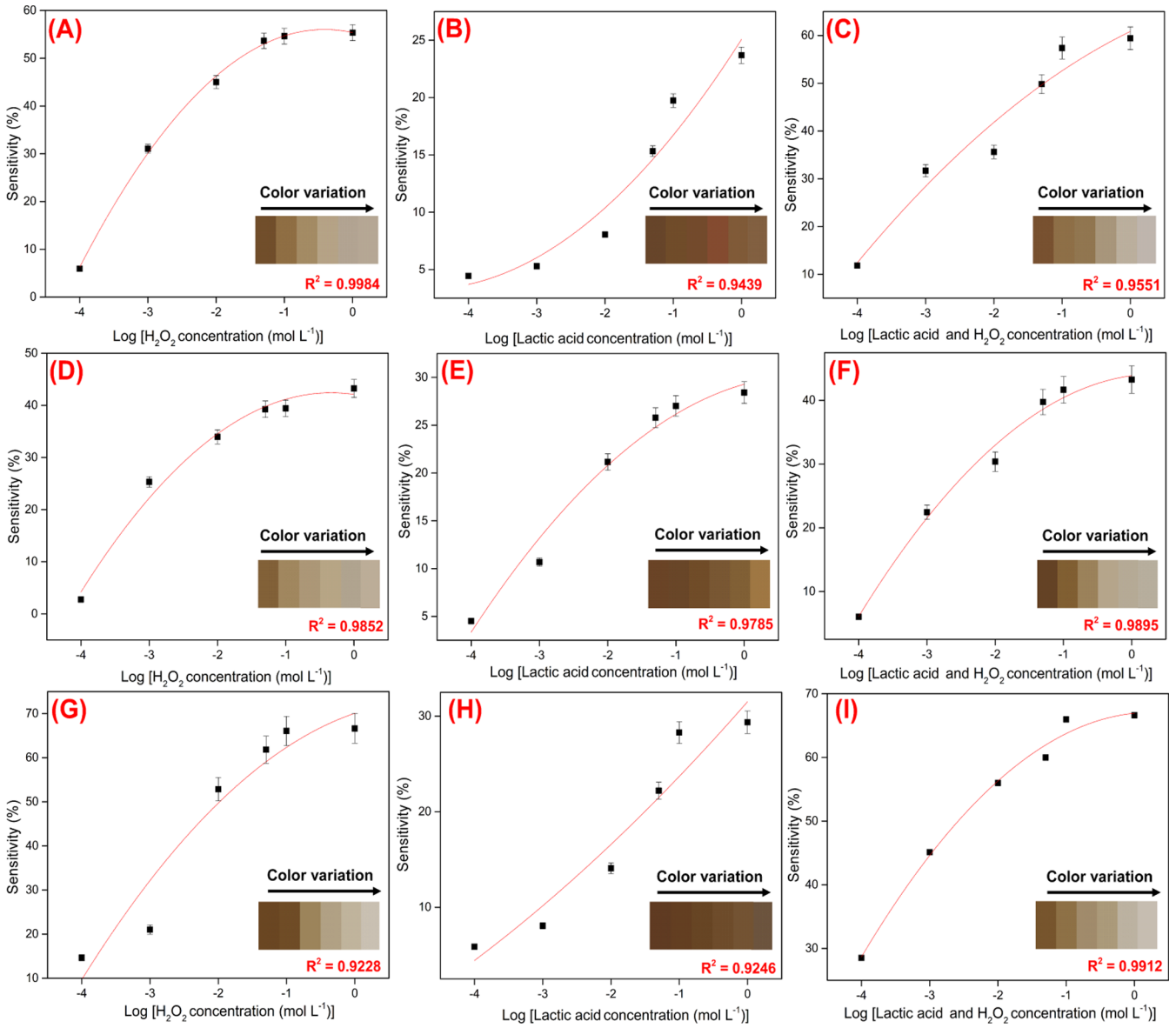

Figure 5. Tests on real whole milk samples: (A) Sensor on the paper substrate for detection of H_2O_2. (B) Sensor on the paper substrate detection of lactic acid. (C) Sensor on the paper substrate for the detection of H_2O_2 and lactic acid. Tests on real low-fat milk samples: (D) Sensor on the paper substrate for detection of H_2O_2. (E) Sensor on the paper substrate for the detection of lactic acid. (F) Sensor on the paper substrate for the detection of H_2O_2 and lactic acid. Tests on real skim milk samples: (G) Sensor on the paper substrate for the detection of H_2O_2. (H) Sensor on the paper substrate for the detection of lactic acid. (I) Sensor on the paper substrate for the detection of H_2O_2 and lactic acid.

concentration of the medium. Therefore, the colorimetric sensor demonstrated dual functionality, serving as a sensor for both the adulterants. No prior literature was found on the dual detection of these adulterants, making this sensor pioneering and innovative for field analyses.

In the FTIR spectrum (Figure 4A), the MnO_2 NSs exhibited two prominent bands in the range of 440−621 cm^{-1}, which was attributed to the elongation of the Mn−O bond.[53] The additional curves represent the sensor spectra before and after the detection of each analyte. Consequently, the three curves exhibited bands at 3281 and 2942 cm^{-1}, corresponding to the elongation of the O−H and N−H bonds found in amino acids.[54] The other bands observed are associated with the presence of amides in zein. Specifically, the band at 1625 cm^{-1} corresponds to the amide I bond, which corresponds to the carbonyl stretch (C═O) of peptide amide groups.[54] The amide II band at 1533 cm^{-1} corresponds to the angular strain vibrations of the N−H bond and C−H stretching vibrations. Furthermore, the amide III band at 1220 cm^{-1} corresponds to the axial strain vibrations of the C−N bond and CO bending vibrations.[54]

Three possible mechanisms were identified in this study (Figure 4B). The first mechanism involves the catalytic decomposition of hydrogen peroxide by MnO_2 NSs, resulting in the release of oxygen and a gradual color change over time.[55] This phenomenon is evident from the band intensity reduction in the range of 440−621 cm^{-1}, corresponding to the presence of MnO_2 NSs in the sensor before and after H_2O_2 detection, as observed in the FTIR spectra (Figure 4C). The second mechanism occurs through the oxidation of the lactic acid by MnO_2 NSs. Previous studies, such as that by Khan et al., have shown that the rate of this noncatalytic reaction pathway is relatively slow.[56] Consequently, only a portion of the nanosheets

https://doi.org/10.1021/acsanm.4c02263
ACS Appl. Nano Mater. 2024, 7, 13701−13711

can undergo reduction, leading to a color change in the sensor, albeit to a lesser extent than H_2O_2. This can be observed by comparing the FTIR bands in the range of 440−621 cm^{-1} across the three curves (Figure 4C). The third mechanism involves a reaction between nonoxidized lactic acid and the amide groups of zein, resulting in an increase in the solubility or degradation of zein.[57] Breaking of the zein chain can occur through interactions with the carboxylic groups of lactic acid. Normally, this process involves hydrolysis, where the peptide bonds that link the amino acids in the zein chain are cleaved by carboxylic acids in the presence of water. This effect is evident from the changes observed in the bands corresponding to amides I, II, and III (from 1625 to 1220 cm^{-1}) in the FTIR spectra (Figure 4C). A similar effect was observed for H_2O_2 detection, albeit to a lesser degree. It is proposed that the intensified sensitivity can be attributed to the ability of the nanosheets to engage in catalytic reactions with peroxide molecules. Conversely, when the nanosheets interacted with lactic acid, a noncatalytic reaction pathway was involved, resulting in a slower reaction rate. Consequently, the sensor exhibited lower sensitivity toward lactic acid as an analyte. The catalytic selectivity of MnO_2 is governed by several factors, including the crystalline structure and morphology of MnO_2.[58,59] The size and shape of MnO_2 particles directly affect their surface area, thereby influencing their capacity for adsorption and reaction.[58] Specifically, the selectivity of MnO_2 NSs toward H_2O_2 stems from the presence of active sites on the MnO_2 surface, which can proficiently adsorb and react with the H_2O_2 molecules. These adsorption sites possess specific dimensions corresponding to the morphology of MnO_2, thus preventing the effective adsorption of larger molecules such as lactic acid.[58] Consequently, MnO_2 did not exhibit significant catalytic activity toward lactic acid.

A series of experiments was carried out to investigate the influence of interfering compounds such as urea, melanin, and formaldehyde. The literature shows that these compounds are frequently used as adulterants.[60−65] To ensure consistent comparisons, the concentrations of these compounds and the target analytes were all set at 1×10^{-2} mol L^{-1}, a value exceeding the permissible limits set by various regulatory agencies.[1,60,66] Figure S5 illustrates the individual color patterns obtained from the sensors fabricated on the paper substrate and the tape. The results show that the sensor does not exhibit selectivity for the studied interferents. However, when the target analytes were considered, the sensor displayed selectivity, demonstrating higher sensitivity toward H_2O_2 than toward lactic acid. These findings support the discussion and the proposed reaction mechanism presented in the preceding sections.

3.4. Detection in Milk Samples. Milk samples (in triplicate for each concentration) were intentionally adulterated by adding six known concentrations of H_2O_2, lactic acid, and an equimolar mixture of both the analytes. Figure 5 displays graphs depicting the percentage sensitivity values for the different concentrations of the analytes, separately or in combination. R^2 values were obtained using a second-degree nonlinear polynomial adjustment. For whole milk samples, the sensors integrated into the paper substrate exhibited R^2 values of 0.9984, 0.9439, and 0.9552 for H_2O_2 detection (Figure 5A), lactic acid detection (Figure 5B), and dual detection (Figure 5C), respectively. Similarly, for semiskimmed milk samples, the sensors integrated into the paper substrate showed R^2 values of 0.9852, 0.9785, and 0.9895 for H_2O_2 detection (Figure 5D), lactic acid detection (Figure 5E), and dual detection (Figure 5F), respectively. In the case of skimmed milk samples, the sensors integrated into the paper substrate exhibited R^2 values of 0.9228, 0.9246, and 0.9912 for H_2O_2 detection (Figure 5G), lactic acid detection (Figure 5H), and dual detection (Figure 5I), respectively. Thus, the sensor demonstrated good sensitivity and linear adjustment for adulterated samples. The overall variation across all samples concerning the addition and recovery of H_2O_2 and lactic acid ranged from 78 to 102%, as calculated based on the percentage of sensitivity. Additionally, a video (Video S1) was created demonstrating the practical application of our method to real samples, featuring the use of a smartphone coupled with a darkroom. The sensor could be exploited either by food surveillance agencies or by end consumers. As demonstrated in the video (Video S1), the person conducting the test uses the sensor as a control strip. The analyst immerses the sensor in the milk sample for 15 min. After this, the analyst removes the sensor and uses the RGB Color Detector application to capture an image and collect RGB color pattern data. A template with variations in RGB color patterns is provided alongside the sensor, allowing the analyst to compare the results and determine whether the milk is contaminated.

4. CONCLUSIONS

Colorimetric sensors based on zein-modified MnO_2 NSs were successfully developed for the detection of H_2O_2 and lactic acid in milk samples. These sensors offer a simple, affordable, and portable method for the rapid detection of these adulterants in milk, helping to address the current demand of food quality and safety for dairy products. The LOD values achieved for the sensors fabricated on the paper substrate and adhesive tape were lower than the permissible limits set by regulatory agencies. The sensors also showed selectivity toward the target analytes, displaying higher sensitivity toward H_2O_2 than for lactic acid. This distinction arises from the combined effects of MnO_2-catalyzed H_2O_2 decomposition and lactic acid oxidation, resulting in a color change. Our sensors offer a breakthrough by simultaneously detecting H_2O_2 and lactic acid in milk samples, a capability that has not been reported before in the literature. While acknowledging the trade-off in analytical precision compared to traditional methods, our approach offers advantages in terms of affordability, ease of use, and portability. These combined features make the sensor suitable for on-site analysis, not only for milk but potentially for a wide range of other food products.

■ ASSOCIATED CONTENT

Supporting Information

The Supporting Information is available free of charge at https://pubs.acs.org/doi/10.1021/acsanm.4c02263.

Sensitivity to H_2O_2 in relation to the number of applied layers of zein-MnO_2, EDS analysis of the MnO_2 sheets, paper substrate sensor, sensor after detection of H_2O_2, and sensor after detection of lactic acid, TGA of the MnO_2 NSs, zein, paper, and sensor on the paper substrate, and variation in sensitivity as a function of H_2O_2 concentration (PDF)

Practical application of our method to real samples using the sensor as a control strip (MP4)

■ AUTHOR INFORMATION

Corresponding Author

Daniel Souza Correa − *Nanotechnology National Laboratory for Agriculture (LNNA), Embrapa Instrumentação, 13560-*

https://doi.org/10.1021/acsanm.4c02263
ACS Appl. Nano Mater. 2024, 7, 13701−13711

970 São Carlos, SP, Brazil; PPGQ, Department of Chemistry, Center for Exact Sciences and Technology, Federal University of São Carlos (UFSCar), 13565-905 São Carlos, SP, Brazil; orcid.org/0000-0002-5592-0627; Email: daniel.correa@embrapa.br

Authors

Tamires dos Santos Pereira − *Nanotechnology National Laboratory for Agriculture (LNNA), Embrapa Instrumentação, 13560-970 São Carlos, SP, Brazil; PPGQ, Department of Chemistry, Center for Exact Sciences and Technology, Federal University of São Carlos (UFSCar), 13565-905 São Carlos, SP, Brazil;* orcid.org/0000-0001-5241-5521

Danilo Martins dos Santos − *Nanotechnology National Laboratory for Agriculture (LNNA), Embrapa Instrumentação, 13560-970 São Carlos, SP, Brazil;* orcid.org/0000-0002-3884-3236

Rafaela da Silveira Andre − *Nanotechnology National Laboratory for Agriculture (LNNA), Embrapa Instrumentação, 13560-970 São Carlos, SP, Brazil;* orcid.org/0000-0002-6477-5126

Complete contact information is available at: https://pubs.acs.org/10.1021/acsanm.4c02263

Funding

The Article Processing Charge for the publication of this research was funded by the Coordination for the Improvement of Higher Education Personnel - CAPES (ROR identifier: 00x0ma614).

Notes

The authors declare no competing financial interest.

■ ACKNOWLEDGMENTS

The authors acknowledge the financial support from Fundação de Amparo à Pesquisa do Estado de São Paulo (FAPESP) (Grant numbers: 2018/22214-6, 2016/23793-4, 2017/20973-4, and 2020/10048-4), Conselho Nacional de Desenvolvimento Científico e Tecnológico, and Rede Agronano (Embrapa) from Brazil.

■ REFERENCES

(1) Nagraik, R.; Sharma, A.; Kumar, D.; Chawla, P.; Kumar, A. P. Milk Adulterant Detection: Conventional and Biosensor Based Approaches: A Review. *Sens. Biosensing Res.* **2021**, *33*, No. 100433.

(2) Food and Agriculture Organization of the United Nations (FAO). *Dairy Market Review Emerging Trends and Outlook*; FAO, 2022.

(3) Veríssimo, M. I.; Gamelas, J. A. F.; Fernandes, A. J. S.; Evtuguin, D. V.; Gomes, M. T. S. R. A New Formaldehyde Optical Sensor: Detecting Milk Adulteration. *Food Chem.* **2020**, *318*, No. 126461.

(4) Singh, P.; Gandhi, N. Milk Preservatives and Adulterants: Processing, Regulatory and Safety Issues. *Food Rev. Int.l* **2015**, *31* (3), 236−261.

(5) Juven, B. J.; Pierson, M. D. Antibacterial Effects of Hydrogen Peroxide and Methods for Its Detection and Quantitation. *J. Food Prot.* **1996**, *59* (11), 1233−1241.

(6) Abrantes, M. R.; Da, C.; Campêlo, S.; Berg, J.; Silva, A. D. Fraude Em Leite: Métodos de Detecção e Implicações Para o Consumidor. *Rev. Inst. Adolfo Lutz* **2014**, *73* (3), 244−251.

(7) Nascimento, C. F.; Santos, P. M.; Pereira-Filho, E. R.; Rocha, F. R. P. Recent Advances on Determination of Milk Adulterants. *Food Chem.* **2017**, *221*, 1232−1244.

(8) Abbas, M. E.; Luo, W.; Zhu, L.; Zou, J.; Tang, H. Fluorometric Determination of Hydrogen Peroxide in Milk by Using a Fenton Reaction System. *Food Chem.* **2010**, *120* (1), 327−331.

(9) Liu, H.; Ding, Y.; Yang, B.; Liu, Z.; Liu, Q.; Zhang, X. Colorimetric and Ultrasensitive Detection of H2O2 Based on Au/Co3O4-CeOx Nanocomposites with Enhanced Peroxidase-like Performance. *Sens Actuators, B* **2018**, *271*, 336−345.

(10) Pi, J.; Bai, Y.; Zhang, Q.; Wong, V.; Floering, L. M.; Daniel, K.; Reece, J. M.; Deeney, J. T.; Andersen, M. E.; Corkey, B. E.; Collins, S. Reactive Oxygen Species as a Signal in Glucose-Stimulated Insulin Secretion. *Diabetes* **2007**, *56* (7), 1783−1791.

(11) Barnham, K. J.; Masters, C. L.; Bush, A. I. Neurodegenerative Diseases and Oxidative Stress. *Nat. Rev. Drug Discovery* **2004**, *3* (3), 205−214.

(12) Fruehauf, J. P.; Meyskens, F. L. Reactive Oxygen Species: A Breath of Life or Death? *Clin. Cancer Res.* **2007**, *13* (3), 789−794.

(13) Finkel, T.; Serrano, M.; Blasco, M. A. The Common Biology of Cancer and Ageing. *Nature* **2007**, *448* (7155), 767−774.

(14) Pravda, J. Hydrogen Peroxide and Disease: Towards a Unified System of Pathogenesis and Therapeutics. *Mol. Med.* **2020**, *26* (1), No. 41, DOI: 10.1186/s10020-020-00165-3.

(15) Hu, X.; Zhang, X.; Li, Y.; Shi, J.; Huang, X.; Li, Z.; Zhang, J.; Li, W.; Xu, Y.; Zou, X. Easy-to-Use Visual Sensing System for Milk Freshness, Sensitized with Acidity-Responsive N-Doped Carbon Quantum Dots. *Foods* **2022**, *11* (13), No. 1855, DOI: 10.3390/foods11131855.

(16) Coelho, M. C.; Malcata, F. X.; Silva, C. C. G. Lactic Acid Bacteria in Raw-Milk Cheeses: From Starter Cultures to Probiotic Functions. *Foods* **2022**, *11* (15), No. 2276.

(17) Lakade, A. J.; Sundar, K.; Shetty, P. H. Nanomaterial-Based Sensor for the Detection of Milk Spoilage. *LWT–Food Sci. Technol.* **2017**, *75*, 702−709.

(18) Terra, I.; Mercante, L.; Andre, R.; Correa, D. Fluorescent and Colorimetric Electrospun Nanofibers for Heavy-Metal Sensing. *Biosensors* **2017**, *7* (4), 61.

(19) Yang, F. Q.; Ge, L. Colorimetric Sensors: Methods and Applications. *Sensors* **2023**, *23* (24), 9887.

(20) Carneiro, S. V.; Oliveira, J. J. P.; Rodrigues, V. S. F.; Fechine, L. M. U. D.; Antunes, R. A.; Neto, M. L. A.; De Moura, T. A.; César, C. L.; De Carvalho, H. F.; Paschoal, A. R.; Freire, R. M.; Fechine, P. B. A. Doped Carbon Quantum Dots/PVA Nanocomposite as a Platform to Sense Nitrite Ions in Meat. *ACS Appl. Mater. Interfaces* **2022**, *14* (38), 43597−43611.

(21) Facure, M. H. M.; Schneider, R.; Mercante, L. A.; Correa, D. S. A Review on Graphene Quantum Dots and Their Nanocomposites: From Laboratory Synthesis towards Agricultural and Environmental Applications. *Environ. Sci. Nano* **2020**, *7* (12), 3710−3734.

(22) Silah, H.; Demir, E.; Yıldırım, S.; Uslu, B. Carbon Nanomaterial-Based Sensors for the Development of Sensitive Sensor Platform. In *Carbon Nanomaterials-Based Sensors*; Elsevier, 2022; pp 191−246.

(23) Correa, D. S.; Pavinatto, A.; Mercante, L. A.; Mattoso, L. H. C.; Oliveira, J. E.; Riul, A. Chemical Sensors Based on Hybrid Nanomaterials for Food Analysis. In *Nanobiosensors*; Academic Press, 2017; pp 205−244.

(24) Schneider, R.; Facure, M. H. M.; Chagas, P. A. M.; Andre, R. S.; dos Santos, D. M.; Correa, D. S. Tailoring the Surface Properties of Micro/Nanofibers Using 0D, 1D, 2D, and 3D Nanostructures: A Review on Post-Modification Methods. *Adv. Mater. Interfaces* **2021**, *8* (13), No. 2100430.

(25) Zhu, D.; Liu, B.; Wei, G. Two-Dimensional Material-Based Colorimetric Biosensors: A Review. *Biosensors* **2021**, *11* (8), 259.

(26) Geleta, G. S. A Colorimetric Aptasensor Based on Two Dimensional (2D) Nanomaterial and Gold Nanoparticles for Detection of Toxic Heavy Metal Ions: A Review. *Food Chem. Adv.* **2023**, *2*, No. 100184.

(27) Sun, Y.; Wang, Y.; Liu, Y.; Wang, H.; Yang, C.; Liu, X.; Wang, F. Integration of Manganese Dioxide-Based Nanomaterials for Biomedical Applications. *Adv. NanoBiomed Res.* **2023**, *3* (1), No. 2200093.

(28) Qian, Z.; Tan, R.; Zhang, X.; Leng, Y.; Chen, Z. MnO2 Nanosheet-Based Colorimetric Sensor Array: Toward Identification of Organophosphorus Pesticides. *Microchem. J.* **2022**, *181*, No. 107758.
(29) Wang, Q.; Ma, X.; Lv, H.; Wei, A.; Wu, T.; Ding, L.; Ma, X.; Ma, C. MnO2 Nanoparticle Mediated Colorimetric Turn-off Determination of Ascorbic Acid. *New J. Chem.* **2020**, *44* (2), 381−386.
(30) Wu, M.; Hou, P.; Dong, L.; Cai, L.; Chen, Z.; Zhao, M.; Li, J. Manganese Dioxide Nanosheets: From Preparation to Biomedical Applications. *Int. J. Nanomed.* **2019**, *14*, 4781.
(31) Zhang, G.; Zhang, J.; Yang, H.; Li, X. In-Situ Redox Reaction Derived Porous Nanosheets of MnO2 for Supercapacitors. *Mater. Lett.* **2022**, *306*, No. 130858.
(32) Huang, Z.; Yang, J.; Zhang, L.; Geng, X.; Ge, J.; Hu, Y.; Li, Z. A Novel One-Step Colorimetric Assay for Highly Sensitive Detection of Glucose in Serum Based on MnO2 Nanosheets. *Anal. Methods* **2017**, *9* (29), 4275−4281.
(33) Huang, Z.; Zheng, L.; Feng, F.; Chen, Y.; Wang, Z.; Lin, Z.; Lin, X.; Weng, S. A Simple and Effective Colorimetric Assay for Glucose Based on MnO2 Nanosheets. *Sensors* **2018**, *18* (8), 2525.
(34) Vahedikia, N.; Garavand, F.; Tajeddin, B.; Cacciotti, I.; Jafari, S. M.; Omidi, T.; Zahedi, Z. Biodegradable Zein Film Composites Reinforced with Chitosan Nanoparticles and Cinnamon Essential Oil: Physical, Mechanical, Structural and Antimicrobial Attributes. *Colloids Surf., B* **2019**, *177*, 25−32.
(35) Bocanegra-Rodríguez, S.; Jornet-Martínez, N.; Molins-Legua, C. Campíns-Falcó, P. Delivering Inorganic and Organic Reagents and Enzymes from Zein and Developing Optical Sensors. *Anal. Chem.* **2018**, *90* (14), 8501−8508.
(36) Latorre-Sanchez, A.; Pomposo, J. A. A Simple, Fast and Highly Sensitive Colorimetric Detection of Zein in Aqueous Ethanol via Zein−Pyridine−Gold Interactions. *Chem. Commun.* **2015**, *51* (86), 15736−15738.
(37) Sinha, A. K.; Pradhan, M.; Pal, T. Morphological Evolution of Two-Dimensional MnO2 Nanosheets and Their Shape Transformation to One-Dimensional Ultralong MnO2 Nanowires for Robust Catalytic Activity. *J. Phys. Chem. C* **2013**, *117* (45), 23976−23986.
(38) Ezati, P.; Rhim, J. W. PH-Responsive Pectin-Based Multifunctional Films Incorporated with Curcumin and Sulfur Nanoparticles. *Carbohydr. Polym.* **2020**, *230*, No. 115638.
(39) RGB Color Detector—Apps on Google Play, 2023. https://play.google.com/store/apps/details?id=com.TheProgrammer.RGBColorDetector&hl=en_US&gl=US.
(40) Code of Federal Regulations. Direct Food Substances Affirmed as Generally Recognized as Safe, 2023. https://www.ecfr.gov/current/title-21/chapter-I/subchapter-B/part-184?toc=1.
(41) Agência Nacional de Vigilância Sanitária. Informe no 34 de 2007, 2023. https://www.gov.br/anvisa/pt-br/assuntos/alimentos/informes/copy_of_34de2007.
(42) Lima, L. S.; Rossini, E. L.; Pezza, L.; Pezza, H. R. Bioactive Paper Platform for Detection of Hydrogen Peroxide in Milk. *Spectrochim. Acta, Part A* **2020**, *227*, No. 117774.
(43) Oaki, Y.; Imai, H. One-Pot Synthesis of Manganese Oxide Nanosheets in Aqueous Solution: Chelation-Mediated Parallel Control of Reaction and Morphology. *Angew. Chem., Int. Ed.* **2007**, *46* (26), 4951−4955.
(44) Heydari, M.; Yousefi, A. R.; Nikfarjam, N.; Rahdar, A.; Kyzas, G. Z.; Bilal, M. Plant-Based Nanoparticles Prepared from Protein Containing Tribenuron-Methyl: Fabrication, Characterization, and Application. *Chem. Biol. Technol. Agric.* **2021**, *8* (1), No. 53.
(45) Silva, S. C. M.; Fuzatto, R. H. S.; Botrel, D. A.; Ugucioni, J. C.; Oliveira, J. E. Development of Zein Nanofibers for the Controlled Delivery of Essential Amino Acids for Fish Nutrition. *SN Appl. Sci.* **2020**, *2* (11), No. 1783.
(46) Naderi, H. R.; Reza Ganjali, M.; Norouzi, P. The Study of Supercapacitive Stability of MnO2/MWCNT Nanocomposite Electrodes by Fast Fourier Transformation Continues Cyclic Voltammetry. *Int. J. Electrochem. Sci.* **2016**, *11* (6), 4267−4282.
(47) Sun, G.; Jia, C.; Zhang, J.; Hou, L.; Ma, Z.; Shao, G.; Wang, Z. B. Core-Shell Structure LiNi1/3Mn1/3Co1/3O2@ Ultrathin δ-MnO2 Nanoflakes Cathode Material with High Electrochemical Performance for Lithium-Ion Batteries. *Ionics* **2019**, *25* (11), 5249−5258.
(48) Yu, P.; Yu, H.; Sun, Q.; Ma, B. Filter Paper Supported NZVI for Continuous Treatment of Simulated Dyeing Wastewater. *Sci. Rep.* **2019**, *9* (1), No. 11322.
(49) Zhang, Q.; Han, X.; Pu, J. Formaldehyde Adsorption Composite Paper with Nacre-Inspired Structure and High Mechanical Strength Properties. *Appl. Phys. A: Mater. Sci. Process.* **2019**, *125* (7), No. 453.
(50) Rattu, G.; Murali Krishna, P. Enzyme-Free Colorimetric Nanosensor for the Rapid Detection of Lactic Acid in Food Quality Analysis. *J. Agric. Food Res.* **2022**, *7*, No. 100268.
(51) Zhang, L.; Hou, W.; Lu, Q.; Liu, M.; Chen, C.; Zhang, Y.; Yao, S. Colorimetric Detection of Hydrogen Peroxide and Lactate Based on the Etching of the Carbon Based Au-Ag Bimetallic Nanocomposite Synthesized by Carbon Dots as the Reductant and Stabilizer. *Anal. Chim. Acta* **2016**, *947*, 23−31.
(52) Sharma, L.; Gouraj, S.; Raut, P.; Tagad, C. Development of a Surface-Modified Paper-Based Colorimetric Sensor Using Synthesized Ag NPs-Alginate Composite. *Environ. Technol.* **2021**, *42* (22), 3441−3450.
(53) Qu, F.; Sun, Y.; Guo, S.; Yan, H.; You, J. Fluorescent Detection of 2,4-Dichlorophenoxyacetic Acid in Food Samples Based on Covalent Organic Frameworks and MnO2 Nanosheets. *Food Anal. Methods* **2020**, *13* (10), 1842−1851.
(54) Miao, Y.; Yang, R.; Deng, D. Y. B.; Zhang, L. M. Poly(L-Lysine) Modified Zein Nanofibrous Membranes as Efficient Scaffold for Adhesion, Proliferation, and Differentiation of Neural Stem Cells. *RSC Adv.* **2017**, *7* (29), 17711−17719.
(55) Dos Santos, D. M.; Dias, L. M.; Surur, A. K.; De Moraes, D. A.; Pavarina, A. C.; Fontana, C. R.; Correa, D. S. Electrospun Composite Bead-on-String Nanofibers Containing CaO2Nanoparticles and MnO2Nanosheets as Oxygen-Release Systems for Biomedical Applications. *ACS Appl. Nano Mater.* **2022**, *5* (10), 14425−14436.
(56) Khan, Z.; Raju; Akram, M.; Kabir-Ud-Din. Oxidation of Lactic Acid by Water Soluble (Colloidal) Manganese Dioxide. *Int. J. Chem. Kinet.* **2004**, *36* (6), 359−366.
(57) Lawton, J. W. Zein: A History of Processing and Use. *Cereal Chem.* **2002**, *79* (1), 1−18.
(58) Puspalata, R.; Mal, D.; Amirthapandian, S.; Rangarajan, S. Influence of Structure on Catalytic Activity of Nano-Manganese Oxide. *Radiat. Phys. Chem.* **2020**, *171*, No. 108681.
(59) Yang, J.; Ren, S.; Su, B.; zhou, Y.; Hu, G.; Jiang, L.; Cao, J.; Liu, W.; Yao, L.; Kong, M.; Yang, J.; Liu, Q. Insight into N2O Formation Over Different Crystal Phases of MnO2 During Low-Temperature NH3−SCR of NO. *Catal. Lett.* **2021**, *151* (10), 2964−2971.
(60) Azad, T.; Ahmed, S. Common Milk Adulteration and Their Detection Techniques. *Int. J. Food Contam.* **2016**, *3* (1), No. 22.
(61) Varun, S.; Kiruba Daniel, S. C. G.; Gorthi, S. S. Rapid Sensing of Melamine in Milk by Interference Green Synthesis of Silver Nanoparticles. *Mater. Sci. Eng., C* **2017**, *74*, 253−258.
(62) Song, J.; Wu, F.; Wan, Y.; Ma, L. Colorimetric Detection of Melamine in Pretreated Milk Using Silver Nanoparticles Functionalized with Sulfanilic Acid. *Food Control* **2015**, *50*, 356−361.
(63) Dutta, S. J.; Chakraborty, G.; Chauhan, V.; Singh, L.; Sharanagat, V. S.; Gahlawat, V. K. Development of a Predictive Model for Determination of Urea in Milk Using Silver Nanoparticles and UV−Vis Spectroscopy. *LWT–Food Sci. Technol.* **2022**, *168*, No. 113893.
(64) Mostafapour, S.; Mohamadi Gharaghani, F.; Hemmateenejad, B. Converting Electronic Nose into Opto-Electronic Nose by Mixing MoS2 Quantum Dots with Organic Reagents: Application to Recognition of Aldehydes and Ketones and Determination of Formaldehyde in Milk. *Anal. Chim. Acta* **2021**, *1170*, No. 338654.
(65) Patari, S.; Datta, P.; Mahapatra, P. S. 3D Paper-Based Milk Adulteration Detection Device. *Sci. Rep.* **2022**, *12* (1), No. 13657.
(66) Faria, I. D. L.; Gouvêa, M. M.; Pereira Netto, A. D.; de Carvalho Marques, F. F. Determination of Formaldehyde in Bovine Milk by Micellar Electrokinetic Chromatography with Diode Array Detection. *LWT–Food Sci. Technol.* **2022**, *163*, No. 113473.

https://doi.org/10.1021/acsanm.4c02263
ACS Appl. Nano Mater. 2024, 7, 13701−13711